

ENERGY TRANSFER IN THE PURPLE MEMBRANE OF *HALOBACTERIUM HALOBIUM*

JAMES B. HURLEY AND THOMAS G. EBREY, *Department of Physiology and
Biophysics, University of Illinois, Urbana, Illinois 61801 U.S.A.*

ABSTRACT The absorption spectrum of the primary photoproduct (the bathoproduct, or K) of the purple membrane protein (PM) at -196°C has a maximum at 628 nm and an extinction coefficient of 87,000. Knowing the absorption spectrum allowed us to calculate the quantum efficiencies for PM to K and K to PM conversion at -196°C . Direct measurements of these quantum yields at -196°C gave 0.33 ± 0.05 and 0.67 ± 0.04 , respectively. Determination of relative quantum efficiencies for PM to K and K to PM conversion by analysis of the absorption spectra of several photostationary-state mixtures of PM and K at -196°C , however, gave wavelength-dependent quantum efficiencies that appear to be >1 . These anomalous results can be readily explained in terms of energy transfer from PM to K within the trimer clusters of pigment molecules which exist in the purple membrane. A model for such a transfer predicts an efficiency of energy transfer from PM to K of about 43%.

INTRODUCTION

The purple membrane protein (PM568) of *Halobacterium halobium* utilizes light energy to cycle the protein through a series of intermediates (Fig. 1) which results in the translocation of protons across the membrane (Lozier et al., 1975; Oesterhelt and StoECKENIUS, 1973). The primary photoproduct of light absorption is called the bathoproduct (K) because it absorbs at longer wavelengths than the pigment and is stable at liquid nitrogen temperature where it can be photochemically converted back to the original pigment. Upon illumination at -196°C a photostationary-state mixture of PM and K is produced (Lozier et al., 1975). It is the ground state of the primary photoproduct K which stores the free energy subsequently used in the proton pumping cycle (Rosenfeld et al., 1977). Here we shall deal with the primary photochemistry of the purple membrane, i.e., the photochemical relationship between PM and K. Although other mechanisms have been proposed, there is increasing evidence that, as in rhodopsin, the primary photochemical event is a geometric change of the chromophore, perhaps isomerization about a double bond (Rosenfeld et al., 1977; Aton et al., 1977; Pettei et al., 1977; Hurley et al., 1977).

The purple membrane protein is arranged in the membrane in a two-dimensional crystalline array with P_3 symmetry (Henderson and Unwin, 1975) so that the proteins are grouped into trimers with their chromophores about 15 Å apart, center to center (Ebrey et al., 1977). The strong interaction between the PM molecules suggests that there should be energy transfer of a restricted sort between them (Ebrey et al., 1977).

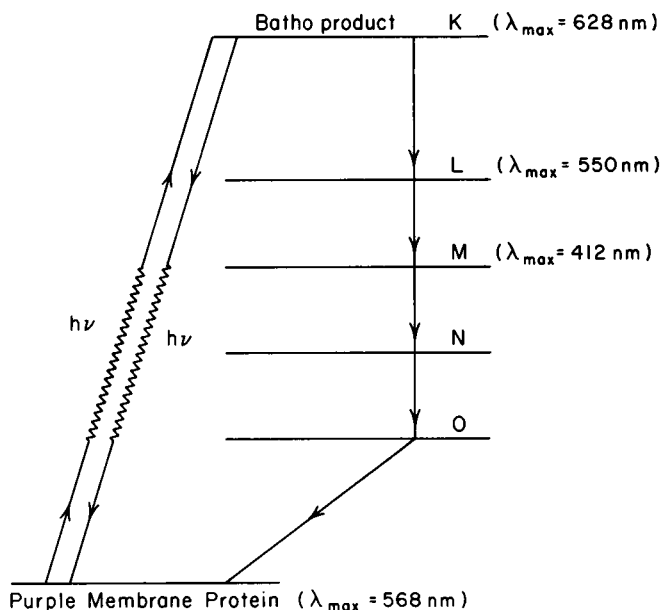


FIGURE 1 Photochemical intermediates of the purple membrane (after Lozier et al., 1975) cycle on a relative free energy scale (see Rosenfeld et al., 1977).

In this paper, we characterize the primary photochemistry of the purple membrane protein at -196°C and study the membrane when a photosteady state is created so that both PM and the bathoproduct K are present. We show that some seemingly anomalous photochemical behavior can be explained in terms of energy transfer from PM to K.

METHODS

Purple membrane of *H. halobium* was isolated according to the method of Becher and Cassim (1975). The fragments were suspended in 2:1 glycerol:water to allow absorption measurements at liquid nitrogen temperature. Optically clear samples were obtained at these temperatures by injection of the sample with a syringe into a 2-mm cell precooled in liquid nitrogen (F. Tokunaga, private communication). Absorption measurements were made through the flat windows of a Dewar flask filled with liquid nitrogen. All absorption measurements were made with a Cary 118 spectrophotometer (Cary Instruments, Fairfield, N.J.).

Absolute quantum efficiencies at -196°C were measured in a flat-windowed Dewar flask using interference filters to isolate selected wavelengths from a tungsten lamp. The fractional amount of K, χ_K , formed at a given time, was calculated from the absorption measured from the digital readout of the spectrophotometer at 640 nm, the maximum in the difference spectrum between K and PM:

$$\chi_K = \frac{\text{OD}_{\text{mix}}^{640} - \text{OD}_{\text{PM}}^{640}}{\text{OD}_{\text{500ss}}^{640} - \text{OD}_{\text{PM}}^{640}} \chi_K^{500\text{ss}} \quad (1)$$

where $\text{OD}_{\text{mix}}^{640}$ = the absorbance at 640 nm of the mixture of PM and K at any given time,

OD_{500ss}^{640} = the absorbance at 640 nm of the 500 nm photosteady mixture, OD_{PM}^{640} = absorbance at 640 nm of PM, and χ_K^{500ss} = the fraction of chromophores that are K in the photostationary state produced by illumination at 500 nm, as determined in Results. According to Dartnall et al. (1936), the quantum efficiency can be related to absorbance changes at the actinic wavelength:

$$\frac{d \ln (10^{A^\lambda} - 1)}{dt} = k I \epsilon^\lambda \phi^\lambda, \quad (2)$$

where A^λ = the absorbance due to the pigment undergoing photochemistry at the actinic wavelength λ , ϵ^λ = the extinction coefficient of the pigment at λ , ϕ^λ = the quantum efficiency at λ , k = a constant, I = the incident intensity of quanta per second per unit area. By bleaching rhodopsin under identical conditions, we can use it as a quantum counter to determine the quantum efficiency of PM568:

$$\phi_{PM} = \frac{\frac{d \ln (10^{A_{PM}^\lambda} - 1)}{dt}}{\frac{d \ln (10^{A_{rh}^\lambda} - 1)}{dt}} \frac{\epsilon_{rh}^\lambda}{\epsilon_{PM}^\lambda} \phi_{rh}, \quad (3)$$

where $\phi_{rh} = 0.70$ in Ammonyx-LO (Onyx Chemical Co., Jersey City, N.J.; Hurley and Ebrey, unpublished results), very close to Dartnall's (1971) $\phi_{rh} = 0.67$ in digitonin. Correction factors proposed by Dartnall et al. (1936) were not used because they were estimated to be negligible. Conversion of PM to K was never more than 5–10% of the steady-state concentration

so that the photochemical back reaction $K \xrightarrow{h\nu} PM$ could be neglected.

Besides the $PM \rightarrow K$ measurements, direct measurement of the quantum efficiency of K to PM conversion was made in photosteady-state mixtures containing both K and PM but at wavelengths where only K absorbed. A photodiode of known spectral sensitivity (EG&G HUV-4000 CAL) was used to determine quantum fluxes at wavelengths longer than where rhodopsin could be used as a quantum counter. Absolute calibration of the photodiode was done with rhodopsin. To measure the rate of K to PM conversion, K was first formed in a 500-nm steady-state mixture at $-196^\circ C$. Quantum efficiencies were determined as above by irradiating at longer wavelengths where there is little or no PM absorption.

Quantum efficiencies of $K \rightarrow PM$ can also be determined at wavelengths where PM absorbs by an analysis of the photostationary state at each irradiating wavelength. In the photostationary state,

$$\phi_{PM}^{\lambda, app} \epsilon_{PM}^\lambda [PM] = \phi_K^{\lambda, app} \epsilon_K^\lambda [K] \quad (4)$$

or

$$\phi_{PM}^{\lambda, app} \epsilon_{PM}^\lambda (1 - \chi_{Kss}^\lambda) = \phi_K^{\lambda, app} \epsilon_K^\lambda \chi_{Kss}^\lambda, \quad (5)$$

where χ_{Kss}^λ = fraction of K in the photostationary state produced by irradiation at λ and can be determined from Eq. 1. We can then find the relative quantum efficiencies:

$$\frac{\phi_{PM}^{\lambda, app}}{\phi_K^{\lambda, app}} = \frac{\epsilon_K^\lambda \chi_{Kss}^\lambda}{\epsilon_{PM}^\lambda (1 - \chi_{Kss}^\lambda)}. \quad (6)$$

Eq. 6 assumes no transfer of energy between PMs and Ks within clusters. It will be shown that

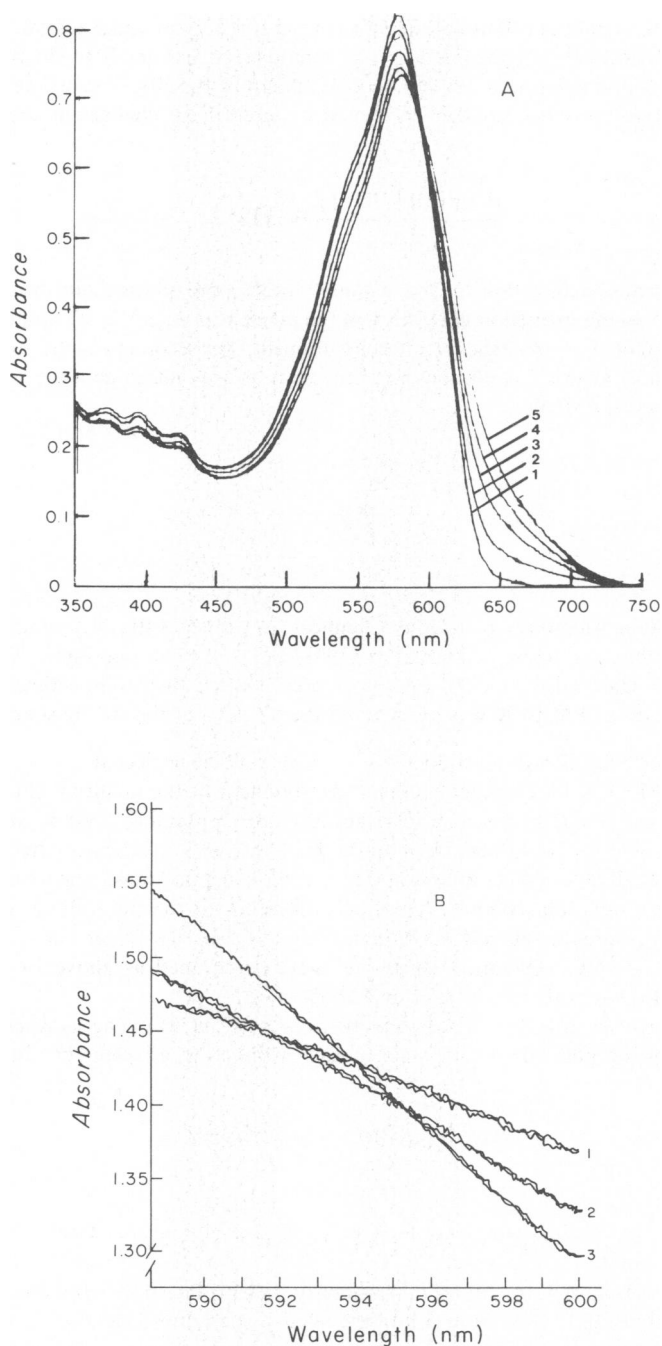


FIGURE 2 (A) Absorption spectra at -196°C of (1) PM568 and of photostationary-state mixtures of PM and K produced by irradiation at (2) 625 nm, (3) 600 nm, (4) 580 nm, (5) 500 nm. (B) Close inspection of the apparent isosbestic point between (1) PM568 and photostationary-state mixtures of PM and K produced by irradiation at (2) 600 nm and (3) 540 nm.

this assumption is not valid. The superscript *app* then refers to the relative apparent quantum efficiencies as calculated from Eq. 6.

RESULTS

Evidence for Energy Transfer

PERCENT OF BATHOPRODUCT K IN A 500-NM PHOTOSTATIONARY STATE Fig. 2 shows the absorption spectra of several photostationary-state mixtures of PM and K produced by irradiation at -196°C . There is a very good (but not exactly perfect, see Fig. 2 B) isosbestic point, indicating that only two major species are present—PM and K. The most K was produced by 500 nm light. If the amount of K in a photostationary state set up by any irradiating wavelength could be determined, then the absorption spectrum of K could be determined and the amount of K in *any* photostationary state easily calculated from Eq. 1.

The composition of the 500-nm photostationary-state mixture of PM and K at -196°C was determined by taking advantage of the complete conversion of irradiated PM568 to M412 at -70°C under conditions of high salt concentration and high pH (Becher and Ebrey, 1977). The samples were made up with 80% glycerol to eliminate the formation of microcrystals at -70°C . The initial spectrum of PM at -70°C was

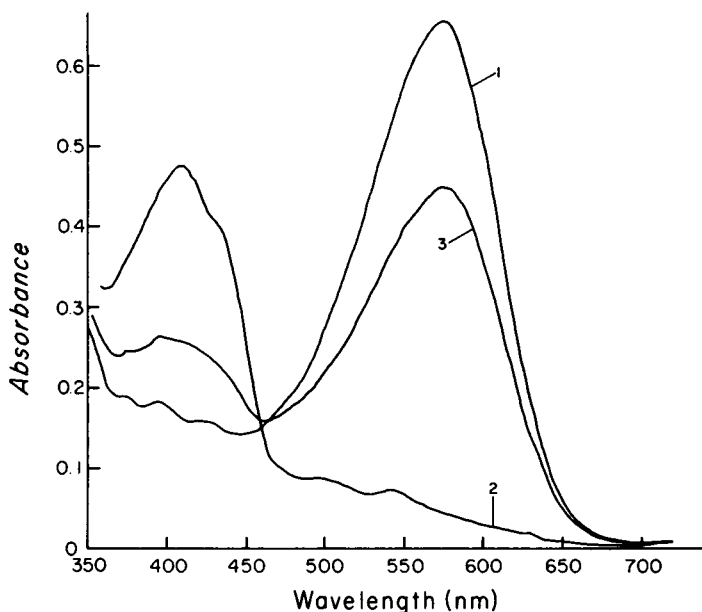


FIGURE 3 Determination of the percent of the bathointermediate K in a 500-nm photostationary state. The sample was in 1–2 M NaCl pH ~ 10.0 – 10.5 to allow complete conversion to M (Becher and Ebrey, 1977). Curve 1 is the initial spectrum of PM568 at -70°C . Curve 2 shows 100% conversion of M412 at -70°C and is used as a base line. Curve 3 represents the amount of PM568 remaining after making the 500-nm photostationary state at -196°C and warming to -70°C .

determined by irradiating the sample to convert it to the light-adapted form, waiting a few minutes to allow the intermediates to decay back to PM, and immersing the sample into a Dewar flask containing ethanol at -70°C . To obtain the base line, the sample was irradiated at 600 nm which converted 100% of the sample to M412, which has no absorption beyond 540 nm. The sample was then warmed, allowed to cycle back to PM, and then immersed in liquid nitrogen. Next, a 12-nm half-band width 500-nm interference filter was used with a tungsten light source to create a photostationary state between PM and K at -196°C . This photosteady state mixture was then placed back in the -70°C ethanol to allow the K that was formed at -196°C to convert to M412. This spectrum was recorded, and conversion to M412 again done to determine the base line of this sample. (Comparison of the two base lines allowed correction for the small scattering changes that occurred.) A determination of the composition of the 500-nm photostationary-state mixture is shown in Fig. 3. From this experiment we can then find

$$\text{percent K} = \frac{\text{OD}_{\lambda}^i - \text{OD}_{\lambda}^f}{\text{OD}_{\lambda}^i}, \quad (7)$$

where OD^i = the initial, base-line-corrected absorbance of PM at -70°C , OD^f = the final, base-line-corrected absorbance of PM after warming the photostationary state to -70°C . An important assumption in this procedure is that all the K formed at -196°C decays to M at -70°C (see Discussion). A comparison of the photosteady-state absorption spectra at -196°C in a separate set of experiments indicated that the condition of high salt concentration and high pH had no effect on the percent of the K intermediate formed by irradiation at -196°C .

Five such experiments gave an average of $28 \pm 3\%$ K in the mixture. The photostationary-state compositions produced by other wavelengths were calculated according to Eq. 1 and are given in Table I.

TABLE I
PERCENT K IN PHOTOSTATIONARY STATES PRODUCED BY
IRRADIATION AT -196°C WITH LIGHT OF WAVELENGTH λ

λ	K in photostationary state
<i>nm</i>	%
500	0.28 ± 0.03
520	0.28
540	0.27
560	0.24
580	0.22
585	0.20
595	0.17
600	0.15
606	0.13
625	0.065

ABSORPTION SPECTRUM OF BATHOPRODUCT K From the absorption of the 500-nm photostationary mixture at -196°C , the absorption spectrum of K can be calculated:

$$\text{OD}_K^{\lambda} = \frac{\text{OD}_{\text{mix}}^{\lambda} - (1 - \chi_K^{500\text{ss}})\text{OD}_{\text{PM}}^{\lambda}}{\chi_K^{500\text{ss}}}, \quad (8)$$

where $\text{OD}_{\text{mix}}^{\lambda}$ = absorbance of the 500-nm photostationary-state mixture at -196°C at wavelength λ , $\text{OD}_{\text{PM}}^{\lambda}$ = absorbance of PM at -196°C at λ , and $\chi_K^{500\text{ss}}$ = the fraction of chromophores that are K in the 500-nm photostationary state. These absorbances were corrected for solvent contraction and for scattering by using a base line of the same concentration of purple membrane bleached with light in the presence of hydroxylamine. Based on an extinction coefficient of $63,000 \text{ M}^{-1} \text{ cm}^{-1}$ (Oesterhelt and Hess, 1973) for the light-adapted purple membrane at room temperature, we found that purple membrane has an extinction of 67,000 at -196°C . K was found to have an extinction coefficient of $87,000 \pm \sim 7,000$ at its λ_{max} of $628 \pm \sim 5 \text{ nm}$ (Fig. 4).

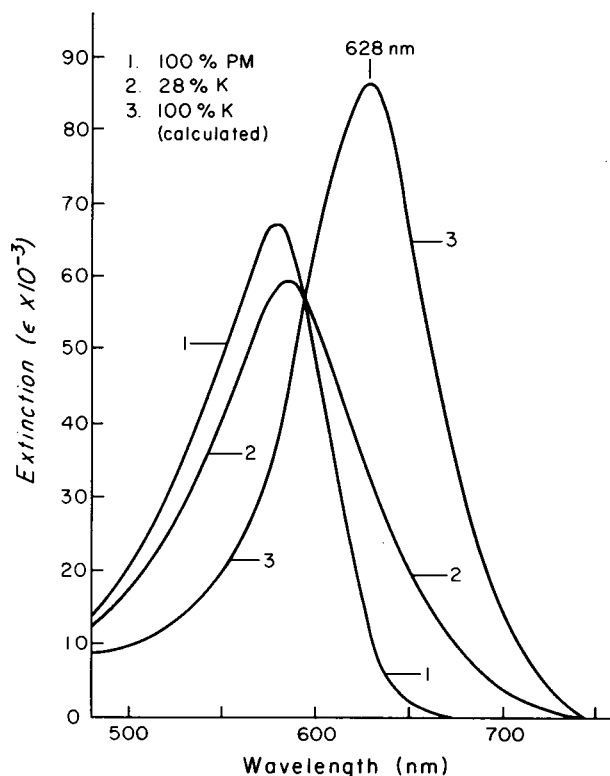


FIGURE 4 Absorption spectrum of the bathintermediate at -196°C . Curves 1 and 2 are the absorption spectra of PM568 and the 500-nm photostationary-state mixture of PM and K corrected for light scattering. Curve 3, the spectrum of K, was calculated according to Eq. 8. The λ_{max} is at 628 nm.

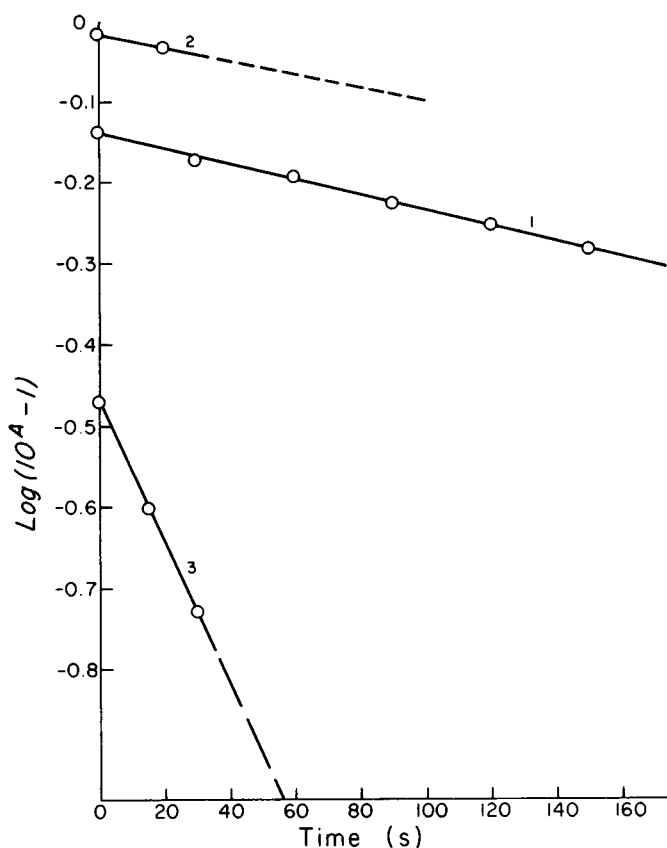


FIGURE 5 Typical experiment showing the determination of photosensitivities of (1) rhodopsin at room temperature with 540 nm light, and (2) PM to K conversion with 540 nm light at -196°C ; (3) K to PM conversion at -196°C at 640 nm. The ratio of quantum intensities at 640–540 nm was 3.24. The two points in curve 2 represent the average of three experiments. The errors in these measurements are less than the symbol sizes. Each photosensitivity relative to that of rhodopsin was repeated from three to six times for each irradiation wavelength. The uncertainty of the slopes and the variance from experiment to experiment are reflected in the errors given in Table II.

TABLE II
QUANTUM EFFICIENCIES FOR PM TO K AND K TO PM CONVERSION
DETERMINED DIRECTLY AT 77°K

λ	$\phi_{\text{PM} \rightarrow \text{K}}$	$\phi_{\text{K} \rightarrow \text{PM}}$	Number of experiments
<i>nm</i>			
520	0.35 ± 0.07	—	4
540	0.34 ± 0.04	—	6
560	0.28 ± 0.02	—	3
640	—	0.63 ± 0.06	4
680	—	0.70 ± 0.02	3

QUANTUM YIELDS FOR $PM \rightarrow K$ AND $K \rightarrow PM$: EVIDENCE FOR ENERGY TRANSFER Absolute quantum yields for the $PM \rightarrow K$ photoconversion calculated as described in Methods are shown in Fig. 5 and Table II. By comparison with measurements at room temperature (Goldschmidt et al., 1976 and 1977) and at -40°C (Becher and Ebrey, 1977), we see that as for rhodopsin (Hurley et al., 1977), these yields are temperature and wavelength independent. This suggests nearly 100% efficient channel-

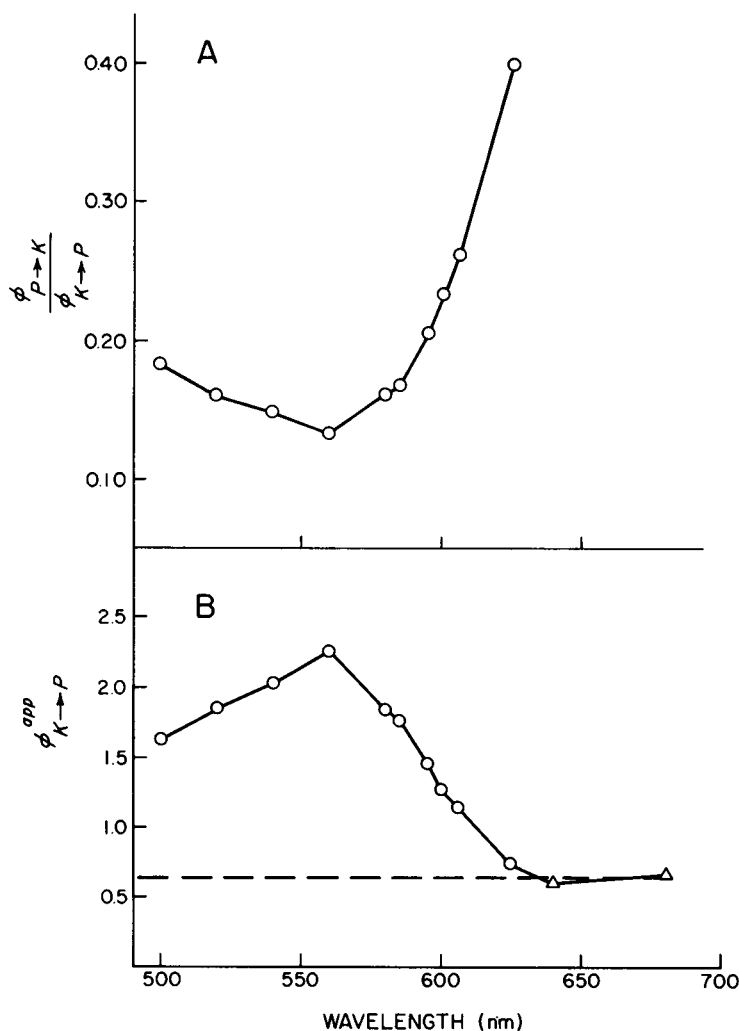


FIGURE 6 (A) The apparent relative quantum efficiencies of $PM \rightarrow K$ and $K \rightarrow PM$ conversion at -196°C at different wavelengths as calculated from Eq. 6. (B) The apparent quantum efficiency of $K \rightarrow PM$ conversion. The triangles (Δ) represent direct measurements; the circles (\circ) represent values calculated from Eqs. 6 and 9. As described in the text, these values do not represent the real quantum efficiency for $K \rightarrow PM$ conversions, shown here by the dashed line (---).

ing of the excited state into a potential minimum common to PM and K (Rosenfeld et al., 1977; Hurley et al., 1977). Relative apparent quantum yields were calculated according to Eq. 6 and are shown in Fig. 6 A. When these values are used to calculate ϕ_K^{app} ,

$$\phi_K^{\lambda, \text{app}} = \frac{\phi_{\text{PM}}}{[\phi_{\text{PM}}^{\lambda, \text{app}} / \phi_K^{\lambda, \text{app}}]}, \quad (9)$$

they yield the results shown in Fig. 6 B. The apparent quantum efficiency is >1 and is strongly wavelength-dependent, suggesting that the above analysis is deficient.

There is a potentially simple explanation of why the apparent quantum efficiency for K to PM conversion is so large and wavelength dependent: that the extinction coefficients used in our calculations were inappropriate because of energy transfer from PM to K. This would give K a larger effective extinction coefficient than that of the isolated pigment.

In the case that includes energy transfer from PM to K the observed photosensitivity of K would be:

$$\phi_K^{\text{app}} \epsilon_K = \phi_K (\epsilon_K + \beta \epsilon_T) \quad (10)$$

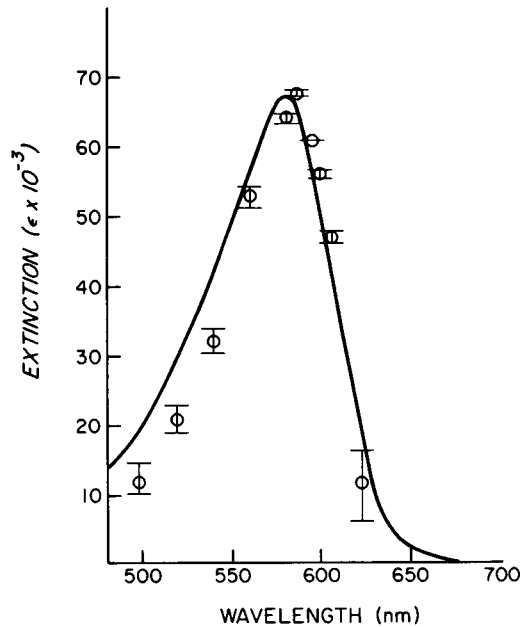


FIGURE 7 Primary evidence for energy transfer from PM to K. The direct proportionality between $\beta \epsilon_T$ (circles) determined according to Eq. 10 and ϵ_{PM} (solid line) is the relationship expected if energy transfer from PM to K occurs. The error bars represent the uncertainties in the base line used in Fig. 4. Uncertainties in the percent K is the 500-nm steady state cause a shift in this curve up or down by about 10% but do not cause major changes in its shape.

where ϕ_K^{app} = the apparent quantum efficiency of $K \rightarrow PM$ conversion calculated from Eq. 9, ϕ_K = the real quantum efficiency of $K \rightarrow PM$ conversion, taken to be 0.7 from measurements at 640 and 680 nm where the PM absorption is negligible, ϵ_T = the extinction coefficient of the species "T" which is transferring energy to K; (presumably, this species is PM), and β is a factor related to the efficiency of transfer of energy from T to K. Solving for $\beta\epsilon_T$ gives

$$\beta\epsilon_T = \epsilon_K \frac{(\phi_K^{app} - \phi_K)}{\phi_K}, \quad (11)$$

which, if the assumption of energy transfer from PM to K is correct, should be roughly proportional to ϵ_{PM} . The proportionality between $\beta\epsilon_T$ and ϵ_{PM} is shown in Fig. 7. This strongly suggests that energy transfer from PM to K is indeed taking place. However, a more comprehensive model is required to quantitate this phenomenon because it would not be expected that β would be totally independent of wavelength.

A Model for Transfer of Energy from PM to K

The complexity of the model describing energy transfer from PM to K arises from the arrangement of the purple membrane molecules within the membrane. The proteins are arranged as trimers in a two-dimensional crystal lattice. As a reasonably tractable, initial model, we consider only the possibility of energy transfer within a trimer; inter-trimer transfer is much less probable but cannot be entirely excluded. To describe the possibilities for energy transfer accurately with our basic model, we must consider each of the four types of clusters found in the photosteady state and labeled a-d in Fig. 8.

AN ESTIMATE OF THE EFFICIENCY OF ENERGY TRANSFER The apparent quantum efficiencies, i.e., the quantum efficiencies that can be determined from Eq. 6 and that would include photoconversion of K back to PM both by light absorbed directly

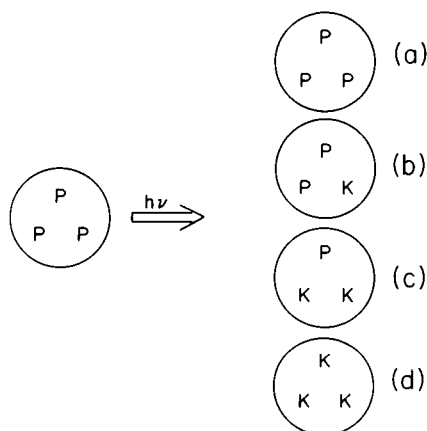


FIGURE 8 Types of trimers produced by irradiation of PM568 at -196°C .

by K and by light absorbed by PM and transferred to K, can be calculated for each of these clusters.

$$\text{for cluster type d } \phi_{K \rightarrow PM}^{app}(d) = \phi_{K \rightarrow PM} = 0.7,$$

$$\text{for cluster type c } \phi_{K \rightarrow PM}^{app}(c) = \phi_{K \rightarrow PM}' 1 + \left(\frac{\alpha}{1 + \alpha} \right) \epsilon_{PM} / \epsilon_K$$

$$\text{for cluster type b } \phi_{K \rightarrow PM}^{app}(b) = \phi_{K \rightarrow PM} [1 + 2\alpha \epsilon_{PM} / \epsilon_K]. \quad (12)$$

For this approximate model, we assume α , the efficiency of energy transfer, is the same for clusters of type b as it is in those of type c. Likewise,

$$\begin{aligned} \phi_{PM \rightarrow K}^{app}(a) &= \phi_{PM \rightarrow K} = 0.3, \\ \phi_{PM \rightarrow K}^{app}(b) &= \phi_{PM \rightarrow K} (1 - \alpha), \\ \phi_{PM \rightarrow K}^{app}(c) &= \phi_{PM \rightarrow K} [1 - 2\alpha / (1 - \alpha)]. \end{aligned} \quad (13)$$

The net apparent quantum efficiencies can then be calculated as functions of α :

$$\phi_{PM}^{app} = \phi_{PM}^{app}(a)G_{PM}(a) + \phi_{PM}^{app}(b)G_{PM}(b) + \phi_{PM}^{app}(c)G_{PM}(c), \quad (14)$$

$$\phi_K^{app} = \phi_K^{app}(b)G_K(b) + \phi_K^{app}(c)G_K(c) + \phi_K^{app}(d)G_K(d), \quad (15)$$

where $G_{PM}(a)$ = the probability of PM being in a type-a cluster, $G_K(b)$ = the probability of a K being in a type-b cluster, etc.

These probabilities can be determined from the distribution of clusters in the photostationary state, e.g.,

$$\begin{aligned} G_{PM}(a) &= \frac{3g(a)}{3g(a) + 2g(b) + g(c)} \\ G_K(b) &= \frac{g(b)}{g(b) + 2g(c) + 3g(d)}. \end{aligned} \quad (16)$$

Here $g(a)$ = the fraction of clusters in the photostationary state which are type a, etc.

Considering the system: (a) \rightleftharpoons (b) \rightleftharpoons (c) \rightleftharpoons (d) in the steady state where $dg(a)/dt = dg(b)/dt = dg(c)/dt = dg(d)/dt = 0$,

$$\begin{aligned} 3\epsilon_{PM}g(a)\phi_{PM}^{app}(a) &= \epsilon_Kg(b)\phi_K^{app}(b), \\ 2\epsilon_{PM}g(b)\phi_{PM}^{app}(b) &= 2\epsilon_Kg(c)\phi_K^{app}(c), \\ \epsilon_{PM}g(c)\phi_{PM}^{app}(c) &= 3\epsilon_Kg(d)\phi_K^{app}(d), \end{aligned} \quad (17)$$

and

$$g(a) + g(b) + g(c) + g(d) = 1. \quad (18)$$

From Eqs. 12, 13, 17, and 18, we can solve for $g(a)$, $g(b)$, and $g(c)$ in terms of α .

TABLE III
EFFICIENCY OF ENERGY TRANSFER FROM PM TO K AT -196°C AND DISTRIBUTION
OF CLUSTER TYPES ACCORDING TO THE MODEL DESCRIBED IN THE TEXT

λ	α^*	$g(a)$	$g(b)$	$g(c)$	$g(d)$
<i>nm</i>					
500	0.34	0.38	0.43	0.17	0.02
520	0.37	0.38	0.42	0.17	0.03
540	0.40	0.40	0.42	0.16	0.02
560	0.47	0.44	0.42	0.13	0.01
580	0.45	0.47	0.41	0.11	0.01
585	0.47	0.50	0.40	0.09	0.01
595	0.47	0.56	0.37	0.06	0.01
600	0.46	0.60	0.35	0.05	0.00
606	0.45	0.65	0.31	0.04	0.00

* α is defined in Eqs. 12 and 13.

These can then be used to express $G_{\text{PM}}(a)$, $G_{\text{PM}}(b) \dots G_{\text{K}}(c)$, $G_{\text{K}}(d)$ as functions of α with Eq. 16, so that the entire expressions for $\phi_{\text{PM}}^{\text{app}}$ and $\phi_{\text{K}}^{\text{app}}$ (Eqs. 14 and 15) are in terms of α . Inasmuch as $[\phi_{\text{PM}}^{\text{app}}/\phi_{\text{K}}^{\text{app}}]$ can be determined experimentally at any wavelength, an equation containing α as a variable was derived as a function of this ratio. α was determined by an iteration method.

Using this model, the efficiency α of energy transfer from PM to K was found to be 0.43 ± 0.05 and shows a small wavelength dependence (Table III). The model presented assumes that (a) back energy transfer from K to PM does not occur, and (b) orientation factors, which ultimately determine the transfer efficiency, are the same in type-b and type-c clusters; that is, α is assumed to be constant.

PREDICTED NONLINEAR BLEACHING RATE An important feature of this model is that it predicts that the net $\phi_{\text{PM}}^{\text{app}}$ and $\phi_{\text{K}}^{\text{app}}$ should depend on the distribution of PMs and Ks within the various clusters, i.e., $G_{\text{PM}}(a)$, $G_{\text{PM}}(b) \dots G_{\text{K}}(d)$. Because these distributions are functions of the amount of K present, the apparent quantum efficiencies should also depend on the amount of K. By analyzing the rate of formation of the photostationary state, we can then test our model.

The rate of formation of K is:

$$\frac{d[\text{K}]}{dt} = \phi_{\text{PM}}^{\text{app}} I(1 - 10^{-A}) \frac{\epsilon_{\text{PM}}[\text{PM}]}{\epsilon_{\text{PM}}[\text{PM}] + \epsilon_{\text{K}}[\text{K}]} - \phi_{\text{K}}^{\text{app}} I(1 - 10^{-A}) \frac{\epsilon_{\text{K}}[\text{K}]}{\epsilon_{\text{PM}}[\text{PM}] + \epsilon_{\text{K}}[\text{K}]}, \quad (19)$$

where I = the incident intensity (per unit area), A = the absorbance of the sample, $[\text{K}]$ and $[\text{PM}]$ = the concentrations of K and PM present at time t , $(1 - 10^{-A})$ = the fraction of incident photons absorbed by the sample. In terms of the fractional concentrations of the chromophores that are K, X_{K} , this becomes

$$\frac{dX_{\text{K}}}{dt} = I \frac{(1 - 10^{-A})}{A} [\epsilon_{\text{PM}}(1 - X_{\text{K}})\phi_{\text{PM}}^{\text{app}} - \epsilon_{\text{K}}X_{\text{K}}\phi_{\text{K}}^{\text{app}}]. \quad (20)$$

This can be rearranged and integrated to give:

$$\ln \frac{[1 - \chi_{K_2}(1 + \epsilon_K \phi_K^{app}/\epsilon_{PM} \phi_{PM}^{app})]}{[1 - \chi_{K_1}(1 + \epsilon_K \phi_K^{app}/\epsilon_{PM} \phi_{PM}^{app})]} = I \frac{(1 - 10^{-4})}{A} [\epsilon_{PM} \phi_{PM}^{app} + \epsilon_K \phi_K^{app}](t_2 - t_1), \quad (21)$$

where χ_{K_1} = the fraction of chromophores that are K at t_1 , χ_{K_2} = the fraction of chromophores that are K at t_2 .

This integration assumes that $(1 - 10^{-4})/A$, ϕ_{PM}^{app} , and ϕ_K^{app} are constant over Δt . Because none of these should be constant according to our model, Eq. 21 is valid only for small changes in the amount of K.

If ϕ_{PM}^{app} and ϕ_K^{app} were indeed strictly constant then we could use the relation

$$(1 + \epsilon_K \phi_K^{app}/\epsilon_{PM} \phi_{PM}^{app}) = 1/\chi_{K_{ss}}, \quad (22)$$

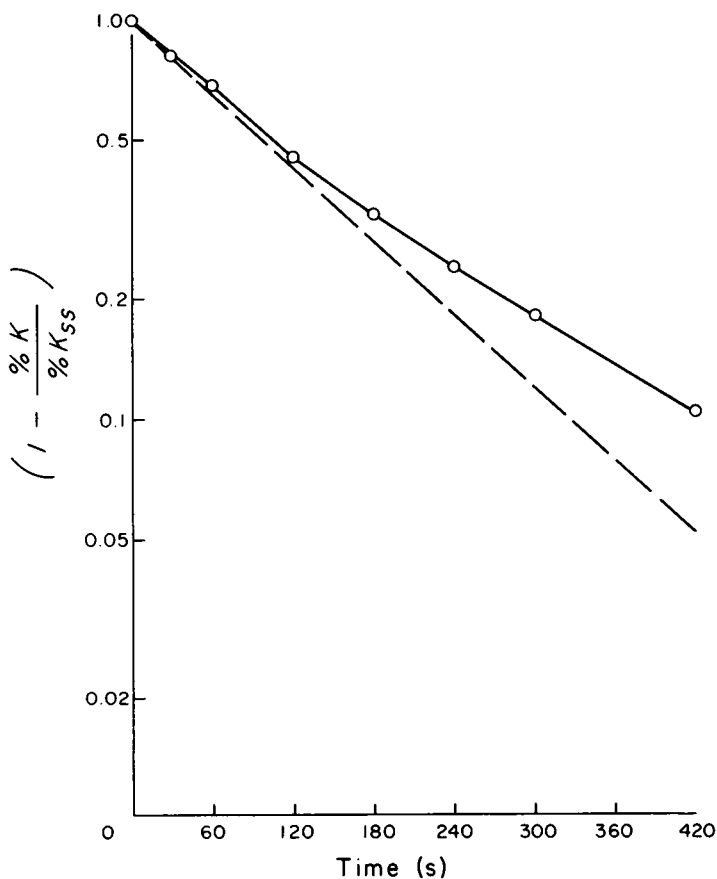


FIGURE 9 Time-course of formation of the 540-nm photostationary state between P and K at -196°C .

where x_{Kss} = the fraction of chromophores that are K in the photostationary state. Then Eq. 21 becomes

$$\ln \frac{(1 - x_{K2}/x_{Kss})}{(1 - x_{K1}/x_{Kss})} = I \frac{(1 - 10^{-A})}{A} [\epsilon_{PM} \phi_{PM}^{app} + \epsilon_K \phi_K^{app}] \Delta t, \quad (23)$$

and by plotting $\ln(1 - x_K/x_{Kss})$ vs. time, a slope that directly proportional to $(1 - 10^{-A}/A)$ should be found. At 540 nm for a sample of absorbance = 0.7, this factor will increase by 13% upon going from $x_K = 0$ to x_{Kss} . Thus, the slope associated with the conversion of PM to K would increase by 13% over the course of the PM \rightarrow K conversion to the photosteady state. However, as shown in Fig. 9, the slope actually decreases by approximately 26%. We conclude from this that ϕ_{PM}^{app} and ϕ_K^{app} are not constant and in fact decrease through the course of the experiment. Thus, our prediction of a nonconstant photosensitivity is confirmed.

The model described above predicts that the apparent quantum efficiencies should decrease, e.g. at 540 nm:

$$\frac{[\epsilon_K \phi_K^{app}(ss) + \epsilon'_{PM} \phi_{PM}^{app}(ss)]}{[\epsilon_K \phi_K^{app}(x_K = 0) + \epsilon_{PM} \phi_{PM}^{app}(x_K = 0)]} = 0.82. \quad (24)$$

However, after a more correct treatment of the data in Fig. 9 in terms of Eq. 21, we find experimentally that this ratio is 0.64 ± 0.08 . Even though our model does qualitatively predict the decrease in the rate of conversion, we do not find exact quantitative agreement.

DISCUSSION

Previous attempts to characterize the photochemistry of purple membrane protein at -196°C have met with serious complications (R. Lozier, personal communication; Hurley and Ebrey, unpublished observations.) Lozier and Niederberger (1977), assuming the quantum efficiencies to be independent of wavelength (Fischer, 1967), calculated the percent K in a 500-nm photostationary-state mixture to be 50%. However, we have found that this assumption does not hold for the purple membrane and its bathoproduct at -196°C . We have bypassed the need to assume that the quantum efficiencies are independent of wavelength by determining the composition of the photostationary state directly under specific conditions that allow the K present in the photostationary state to form a species that does not absorb at the λ_{max} of PM568, M412. From the determination of the percent K in the 500-nm photosteady state, we calculated the absorption spectrum of K. At -196°C the λ_{max} of K is at 628 nm, and we therefore call it K628. Knowing the absorption of K, we could then determine the quantum efficiencies for the K \rightarrow PM conversion.

The quantum efficiencies for photoconversion of PM and K are 0.30 and 0.67, respectively, and show practically no change with temperature. The temperature and wavelength (Table II) independent of the quantum efficiencies, along with the fact that

they sum to one, suggest the existence of a common excited state that can be populated with nearly 100% efficiency from either PM or K (Rosenfeld et al., 1977; footnote 1).

Measurements of the relative quantum yields, at wavelengths where both pigments have significant absorption, gave the quite anomalous results shown in Fig. 6, wavelength-dependent quantum efficiencies that appear to be >1 . However, these results can be readily explained in terms of transfer of excitation from PM to K within the trimer clusters. According to an approximate model, we found that energy is transferred from PM to K with an efficiency of 0.46. The model is qualitatively confirmed by measuring the time-course of formation of the photostationary state, during which the apparent quantum efficiencies should change as the amount of K present increases. As a result of the close proximity of the chromophores within the trimers (Ebrey et al., 1977), it is not unreasonable that energy transfer could occur among chromophores given a favorable orientation within a cluster.

Our determination of the percent K in a photostationary state rests on the assumption that all K formed at -196°C decays to M412 when the sample in high salt, high pH, and 80% glycerol is warmed to -70°C . Experiments are in progress to test this assumption (R. Lozier, personal communication, and F. Tokunaga, personal communication). The outcome of these experiments will determine the validity of the results presented here. However, at this point we feel justified in making this assumption for these reasons: First, the same quantum efficiency is seen for the photoconversion of PM to K at -196°C (this work), and for conversion to M412 at -40°C (Becher and Ebrey, 1977), and at 22°C (Goldschmidt et al., 1977). Second, in support of our value of 28% K in a 500-nm photostationary state, Eqs. 8 and 3 show that values for the percent K in the 500-nm photostationary state larger than 40% would give values for ϕ_K^{640} and ϕ_K^{680} , which are >1.0 . Finally, the magnitude of the decrease in fluorescence seen when a photosteady state is formed would be inconsistent with more than ca. 30% K in the photosteady state (Govindjee et al., 1978).

Analysis by Goldschmidt et al. (1976) of the 530-nm photostationary state produced between PM and K at room temperature showed that the ratio of the quantum yield for conversion of PM to K to that for conversion of K to PM is 0.4. At -196°C from Fig. 6, we find a value of ca. 0.15. This difference can be traced to a quite different absorption spectrum inferred for K at room temperature by Goldschmidt et al. (1976) from the one we determined at -196°C . Further work will be needed to clarify these differences.

The simplified model we have developed here is incomplete, and several questions need to be investigated further. The model assumes that energy transfer from K to PM does not occur. The basis for this assumption is that de-excitation from the thermalized state of K cannot provide enough energy to excite a neighboring PM chromophore. Some direct evidence that certain kinds of back transfer do not occur is given in an accompanying paper (Govindjee et al., 1978). The second assumption in our model is that the relative orientation of the PM and K transition moments is the same in type-b and type-c clusters. Because we do not know the orientation of the transition

moment in K chromophores relative to PM chromophores nor the degree of exciton interaction between Ks in a cluster, this is a necessary simplification. In addition, our model does not consider the possibility of energy transfer among chromophores in different clusters. The lack of precise agreement between the predicted and experimental decrease in slope in the time-course of formation of the photostationary-state experiment suggests that some of these assumptions are not entirely accurate.

Another problem is that when we partially regenerated bleached purple membrane sheets so only 20% of the chromophore sites were occupied (Becher and Ebrey, 1977), we did not see large changes in the efficiency of energy transfer from PM to K (unpublished observations). Such changes probably would be expected if only singly occupied trimers were present and intertrimer transfer did not occur.

A final problem is that PMs and Ks in the various types of clusters might have slightly different absorption spectra. This is suggested by there not being a perfect isosbestic point between different photostationary-state mixtures of PM and K (see Fig. 2 B). These spectral differences probably arise from interactions between the chromophores within the clusters that would yield PM in three different environments (Fig. 8 a-c) and K in three different environments (Fig. 8 b-d). In each case, PM and K would be expected to have very slightly different absorption spectra due to different sets of exciton interactions (Ebrey et al., 1977).

We thank Boryeu Mao, Fumio Tokunaga, Don DeVault, and Brian Becher for many useful conversations. Richard Lozier generously discussed with us his low temperature experiments.

Received for publication 31 August 1977 and in revised form 16 November 1977.

REFERENCES

- ATON, B., A. DOUKAS, R. CALLENDER, B. BECHER, and T. EBREY. 1977. Resonance Raman studies of the purple membrane. *Biochemistry*. **16**:2995.
- BECHER, B., and J. Y. CASSIM. 1975. Improved isolation procedures for the purple membrane of *Halobacterium halobium*. *Prep. Biochem.* **5**:161.
- BECHER, B., and T. G. EBREY. 1977. The quantum efficiency for the photochemical conversion of the purple membrane protein. *Biophys. J.* **17**:185.
- DARTNALL, H. J. A. 1972. Photosensitivity. In *Handbook of Sensory Physiology*. Vol. VII. H. J. A. Dartnall, editor. Springer-Verlag KG, Berlin, W. Germany. 122-145.
- DARTNALL, H. J. A., C. F. GOODEVE, and R. J. LYTHGOE. 1936. The quantitative analysis of the photochemical bleaching of visual purple solutions in monochromatic light. *Proc. Royal Soc. Ser. A. Math. Phy.* **156**:158.
- EBREY, T. G., B. BECHER, B. MAO, P. KILBRIDE, and B. HONIG. 1977. Exciton interactions and chromophore orientation in the purple membrane. *J. Mol. Biol.* **112**:377.
- FISCHER, E. 1967. The calculation of photostationary states in system $A \rightleftharpoons B$ when only A is known. *J. Phys. Chem.* **71**:3704.
- GOLDSCHMIDT, C. R., O. KALISKY, T. ROSENFELD, and M. OTTOLENGHI. 1977. The quantum efficiency of the bacteriorhodopsin photocycle. *Biophys. J.* **17**:179.
- GOLDSCHMIDT, C. R., M. OTTOLENGHI, and R. KORENSTEIN. 1976. On the primary quantum yield in the bacteriorhodopsin photocycle. *Biophys. J.* **16**:839.
- GOVINDJEE, R., B. BECHER, and T. EBREY. 1978. The fluorescence from the chromophore of the purple membrane protein. *Biophys. J.* **22**:67-77.

- HENDERSON, R., and P. N. T. UNWIN. 1975. Three dimensional model of purple membrane obtained by electron microscopy. *Nature (Lond.)*. **257**:28.
- HURLEY, J. B., T. G. EBREY, B. HONIG, and M. OTTOLENGHI. 1977. Temperature and wavelength effects on the photochemistry of rhodopsin, isorhodopsin, bacteriorhodopsin, and their photoproducts. *Nature (Lond.)*. **270**:540.
- LOZIER, R. H., R. A. BOGOMOLNI, and W. STOECKENIUS. 1975. Bacteriorhodopsin: a light-driven proton pump of *Halobacterium halobium*. *Biophys. J.* **15**:955.
- LOZIER, R., and W. NIEDERBERGER. 1977. The photochemical cycle of bacteriorhodopsin. *Fed. Proc.* **36**: 1805.
- OESTERHELT, D., and B. HESS. 1973. Reversible photolysis of the purple complex in the purple membrane of *Halobacterium halobium*. *Eur. J. Biochem.* **37**:316.
- OESTERHELT, D., and W. STOECKENIUS. 1973. Functions of a new photoreceptor membrane. *Proc. Natl. Acad. Sci. U.S.A.* **70**:2853.
- PETTEI, M., A. YUDD, K. NAKANISHI, R. HENSELMAN, and W. STOECKENIUS. 1977. Identification of retinal isomers isolated from bacteriorhodopsin. *Biochemistry*. **16**:1955.
- ROSENFELD, T., B. HONIG, M. OTTOLENGHI, J. B. HURLEY, and T. G. EBREY. 1977. On the role of the protein in the photoisomerization of the visual pigment chromophore. *Pure Appl. Chem.* **49**:341.